# Lasing in a coupled hybrid double quantum dot-resonator system

S. Mojtaba Tabatabaei* and Neda Jahangiri
*Faculty of Physics, Shahid Beheshti University, G. C. Evin, Tehran 1983963113, Iran*

(Received 19 August 2019; revised manuscript received 3 March 2020; accepted 5 March 2020; published 19 March 2020)

We theoretically investigate the possibility of lasing in an electromagnetic resonator coupled to a voltage-biased hybrid double quantum dot comprised of a double quantum dot tunnel coupled simultaneously to a normal metal and a superconducting lead. Using a unitary transformation, we derive a resonator-double quantum dot interaction Hamiltonian in the rotating-wave approximation which reveals the fact that lasing in this system is mediated by electron transitions between Andreev energy levels in the system's density of states. Moreover, by employing a Markovian master equation incorporating dissipation effects for the electronic and photonic degrees of freedom, we numerically calculate the steady-state reduced density matrix of the system from which we determine the average photon number and its statistics in the resonator in various parameter regimes. We find that at some appropriate parameter configurations, lasing can be considerably enhanced due to the possibility of electron transitions between multiple Andreev levels in the system.

DOI: 10.1103/PhysRevB.101.115135

## I. INTRODUCTION

The laser has been one of the most intriguing optical devices over the past few decades, and today, it has found a tremendous number of applications in different fields of science and technology. While in conventional lasers light amplification is induced by optical pumping of a large number of atoms which are weakly coupled to the cavity mode, the realization of a strongly coupled one-atom laser in tightly confined cavity modes is of fundamental interest to researchers due to its particular properties and uses [1–8]. Following the first experimental achievement in 2003 using a single cesium atom strongly coupled to a cavity mode [9], many theoretical proposals and experimental demonstrations were put forward to explore other realizations of single-atom lasers [10–16]. Among these, quantum dot (QD) lasers find a lot of interest because of their tunability as well as their fabrication advantages. In the last two decades, based on the cavity quantum electrodynamics, many micro- and nanocavity lasers with a single QD have been fabricated [17–22].

Recently, similar effects were demonstrated in the circuit quantum electrodynamics architecture, where a double quantum dot (DQD) or a superconducting qubit, which is constantly driven into an excited state by an external electric or magnetic bias, plays the role of an active medium in the electromagnetic resonator formed in a superconducting transmission line [23–32]. In particular, it was theoretically predicted in Ref. [24] and then experimentally shown in Ref. [26] that a voltage-biased DQD can create a lasing state when it is coupled to a resonator through an electric dipole interaction. By noting that it was a DQD coupled to two normal-metal leads which was actually considered in the aforementioned proposals to establish the lasing state in the resonator, it would be valuable to see whether replacing one of the normal-metal leads by a superconductor would have any implications for the lasing behavior.

In general, by coupling a QD to a normal lead and also to a superconducting lead, some new intriguing features arise in the energy configurations and transport properties of the QD, which are basically due to the formation of the resonant Andreev reflections at the QD-superconducting lead interface [33–39]. Recently, the role of such hybrid single QD structures in creating a lasing state in an electromagnetic resonator became attractive [40,41]; however, the consequences of using a hybrid DQD in a voltage-biased DQD laser has not been studied so far. It should be noted that Bruhat *et al.* [42] recently conducted an experiment on a hybrid DQD system coupled to an electromagnetic resonator. They did not study the lasing state in their setup, but instead, they investigated the mechanism of resonator-DQD coupling and observed a symmetric coupling between the hybrid DQD and the resonator which is attributed directly to the roles of superconducting proximity effects in the DQD.

In this paper, we consider a setup comprising a hybrid DQD which is capacitively coupled to an electromagnetic resonator. Using an analytical treatment of the Hamiltonian of the system and also a numerical simulation of the full quantum system in the steady state, we analyze the lasing state in various parameter regimes of this model system. We show that a lasing state with sub-Poissonian statistics is present in this system at frequencies equal to the energy differences between Andreev energy levels in the density of states of the hybrid DQD. There are two Andreev energy levels corresponding to each energy level of the hybrid DQD which are arranged in the density of states (DOS) of the system symmetrically around the chemical potential of the superconducting electrode. Therefore, depending on the weights of different Andreev levels in the DOS, there are some specific parameter regimes for which the system shows lasing due to

*s.m.taba90@gmail.com

 

the electron transitions between the corresponding Andreev energy levels of the hybrid DQD.

The remainder of this paper is organized as follows: In Sec. II, the model Hamiltonian is introduced, and the underlying formalism of the paper is set up. Our numerical results are considered in Sec. III, and conclusions are presented in Sec. IV.

## II. MODEL AND FORMALISM

### A. Model Hamiltonian

As shown in Fig. 1, our model system consists of a hybrid DQD, which is capacitively coupled to a single-mode electromagnetic resonator. The total Hamiltonian of the system can be written as

$$\hat{H} = \hat{H}_{dqd} + \hat{H}_l + \hat{H}_{l-d} + \hat{H}_{\rm ph} + \hat{H}_{ph-dqd}, \tag{1}$$

where $\hat{H}_{dqd}$ is the Hamiltonian of the DQD given by

$$\hat{H}_{dqd} = \sum_\sigma \varepsilon_L \hat{n}_{L,\sigma} + \varepsilon_R \hat{n}_{R,\sigma} + t_d \sum_\sigma (d^\dagger_{R,\sigma} d_{L,\sigma} + \text{H.c.}) + U_R \hat{n}_{R,\uparrow}\hat{n}_{R,\downarrow} + U_L \hat{n}_{L,\uparrow}\hat{n}_{L,\downarrow} + U_{LR}\hat{n}_L\hat{n}_R, \tag{2}$$

where $\hat{n}_{i,\sigma} = \hat{d}^\dagger_{i,\sigma}\hat{d}_{i,\sigma}$ is the electron number operator with spin $\sigma = \uparrow, \downarrow$ in dot $i = L, R$ with energy $\varepsilon_i$ and $t_d$ is the hybridization energy between DQDs. Moreover, $U_L$ and $U_R$ are the on-site Coulomb interaction energies for the left and right dots, respectively, and $U_{LR}$ is the mutual Coulomb interaction between the two dots in the DQD. Furthermore, $\hat{H}_l$ and $\hat{H}_{l-d}$ stand for the Hamiltonian of the leads and tunneling between leads and the DQD, which are given by

$$\hat{H}_l = \sum_{k,\alpha,\sigma} (\varepsilon_{k,\alpha} + \mu_\alpha)\hat{c}^\dagger_{k,\alpha,\sigma}\hat{c}_{k,\alpha,\sigma} + \sum_{k,\alpha} \Delta_\alpha (\hat{c}^\dagger_{k,\alpha,\uparrow}\hat{c}^\dagger_{k,\alpha,\downarrow} + \text{H.c.}), \tag{3}$$

$$\hat{H}_{l-d} = \sum_{k,\alpha,i,\sigma} t_{\alpha,i}(\hat{c}^\dagger_{k,\alpha,\sigma}\hat{d}_{i,\sigma} + \text{H.c.}), \tag{4}$$

where $\hat{c}_\sigma$ denotes the annihilation operator of an electron with spin $\sigma$ in the single-particle state of the left ($\alpha = N$) or right ($\alpha = S$) lead, characterized by the momentum $k$ with energy $\varepsilon_{k,\alpha}$, and $\mu_\alpha$ is the chemical potential of the corresponding lead. Moreover, $\Delta_i$ is the pairing energy gap in the respective lead, which is given by $\Delta_N = 0$ for the normal lead and a real positive $\Delta_S$ for the superconducting lead. Furthermore, $t_{\alpha,i}$ is the tunneling energy between lead $\alpha$ and dot $i$. The left (right) lead is coupled only to the left (right) dot; thus, $t_{N,R} = t_{S,L} = 0$.

Because we are interested in studying the impacts of the presence of superconducting pairing correlations on the lasing behavior in the DQD-resonator coupled system, it is reasonable to consider electronic transitions in the superconducting subgap regime and to disregard the quasiparticle excitations in the continuum region of the superconducting lead. In practice, this is equal to considering a large superconducting gap limit, $\Delta_S \to \infty$, in which all energy scales of the system are smaller than the edges of the superconducting gap. By using a Green's functions description [43] or a Schrieffer-Wolf transformation [44], it can be shown that in this so-called infinite-gap approximation, the superconductor lead is decoupled from the right dot, leaving an effective pairing potential $\Gamma_S(\hat{d}^\dagger_{R,\uparrow}\hat{d}^\dagger_{R,\downarrow} + \text{H.c.})$ in the Hamiltonian of the DQD, where $\Gamma_S = 2\pi|t_{S,R}|^2\rho_0^S$ is the electron tunneling rate between the DQD and the superconducting lead in the wideband approximation and $\rho_0^S$ is the lead's density of states in its normal state. Thus, we can rewrite the Hamiltonian of the DQD as

$$\hat{H}^{SC}_{dqd} = \hat{H}_{dqd} + \Gamma_S(\hat{d}^\dagger_{R,\uparrow}\hat{d}^\dagger_{R,\downarrow} + \text{H.c.}). \tag{5}$$

The Hamiltonian of the single-mode resonator is given by $\hat{H}_{\rm ph} = \hbar\omega_0(\hat{a}^\dagger\hat{a} + \frac{1}{2})$, where $\hat{a}$ is the bosonic annihilation operator of the resonator mode with frequency $\omega_0$. The coupling of the DQD to the resonator is modeled by a capacitive interaction between electrons in the DQD and the electric field in the resonator, and its Hamiltonian is given by

$$\hat{H}_{ph-dqd} = -\sum_{i,\sigma} g_i \hat{n}_{i,\sigma}(\hat{a} + \hat{a}^\dagger), \tag{6}$$

where $g_i$ is the coupling strength between the dot $i$ and the resonator mode.

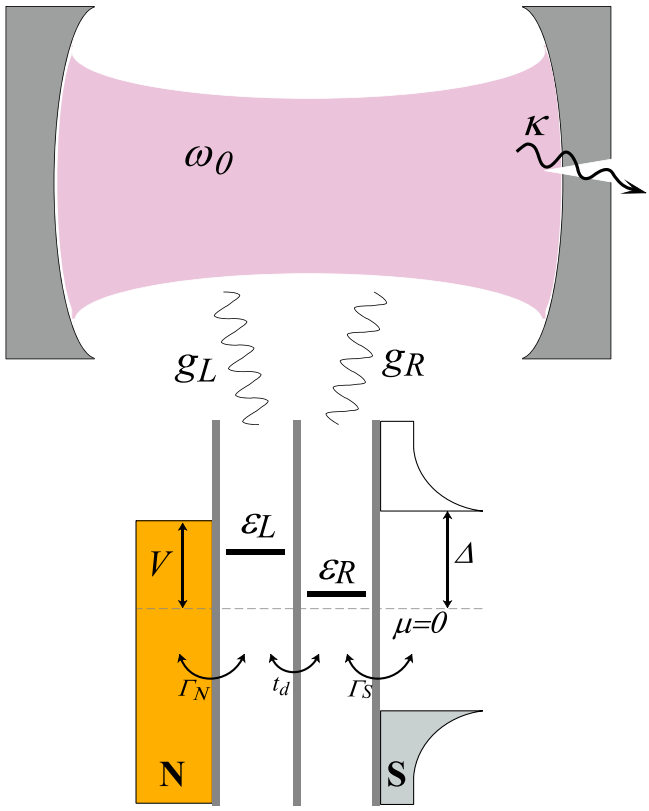


FIG. 1. A single mode resonator is capacitively coupled to a voltage-biased hybrid double quantum dot connected to a normal metal and a superconducting lead.

### B. Master equation description

The coupled DQD-resonator system can be driven into a nonequilibrium state by applying a finite bias voltage $\mu_N = eV_b$ to the normal electrode, where $e$ is the charge of an electron. Following the standard recipe for deriving the master

equation, we consider the DQD-resonator subsystem with the Hamiltonian $\hat{H}_S = \hat{H}^{SC}_{dqd} + \hat{H}_{\rm ph} + \hat{H}_{ph-dqd}$ to be an open system which we seek for its dynamics when it is weakly coupled to the normal-metal electrode and a photon bath. Then, the dynamics of the system can be described by using a master equation of the reduced density matrix $\rho$ of the coupled DQD-resonator system, which in the Markovian approximation is given by [45,46]

$$\frac{d}{dt}\hat{\rho}(t) = -\frac{i}{\hbar}[\hat{H}_S, \hat{\rho}(t)] + \mathcal{L}_{\rm ph}\hat{\rho}(t) + \mathcal{L}_N\hat{\rho}(t), \tag{7}$$

where $\mathcal{L}_{\rm ph}$ and $\mathcal{L}_N$ are, respectively, the Lindblad superoperators describing the dissipation of photons and the electron tunneling between the QD and the normal-metal electrode. While for a general description of the dynamics of the DQD-resonator system, a precise microscopic derivation of the above Lindblad superoperators is necessary, as we are interested here in investigating the possibility of lasing in the hybrid DQD-resonator system, we will focus on situations where the system is at low temperatures and also there is a large bias voltage applied to the normal-metal lead. These assumptions introduce great simplifications in our calculations and allow us to represent the action of the above Lindblad superoperators on the reduced density matrix of the DQD-resonator system by the following forms:

$$\mathcal{L}_{\rm ph}\hat{\rho}(t) = \kappa\left[\hat{a}\hat{\rho}(t)\hat{a}^\dagger - \tfrac{1}{2}\{\hat{a}^\dagger\hat{a}, \hat{\rho}(t)\}\right] \tag{8}$$

and

$$\mathcal{L}_N\hat{\rho}(t) = \Gamma_N \sum_{i,\sigma}\left[\hat{C}_{i\sigma}\hat{\rho}(t)\hat{C}^\dagger_{i\sigma} - \frac{1}{2}\{\hat{C}^\dagger_{i\sigma}\hat{C}_{i\sigma}, \hat{\rho}(t)\}\right], \tag{9}$$

where $\kappa$ is the decay rate of the photons in the resonator, $\Gamma_N = 2\pi|t_{N,L}|^2\rho_0^N$ is the electronic tunneling rate to the normal-metal lead, and $\hat{C}_{i\sigma} = \hat{d}^\dagger_{i,\sigma}$ ($\hat{d}_{i,\sigma}$) for positive (negative) bias voltages. We emphasize that if we had not considered the infinite-gap approximation for the superconducting lead, it would have been necessary in Eq. (7) to consider the effect of coupling to the superconducting lead by introducing its corresponding Lindblad superoperator [47]. We also note that the above formalism best describes the coupled DQD-resonator system when the coupling between the DQD and resonator is weak. For a general treatment in the presence of strong coupling between the DQD and the resonator we can refer to Ref. [46].

By solving Eq. (7) for $d\hat{\rho}(t)/dt = 0$, we obtain the reduced density matrix of the coupled DQD-resonator system in the steady state, from which we can calculate the average value of every observable of the system using the relation $\langle\hat{O}(t)\rangle = {\rm Tr}[\hat{O}\hat{\rho}(t)]$, where ${\rm Tr}[\cdots]$ is the trace with respect to all degrees of freedom in the system. Of interest to us here are the average photon number $n_{\rm photon} = \langle a^\dagger a\rangle$ and the Fano factor of the photons, where the latter can be calculated by the relation $F = (\langle a^\dagger a a^\dagger a\rangle - \langle a^\dagger a\rangle^2)/\langle a^\dagger a\rangle$. The Fano factor can be referred to as a means to distinguish between the photon bunching ($F > 1$) or antibunching ($F < 1$) regimes and describes whether the photons inside the resonator have either sub-Poissonian ($F < 1$), Poissonian ($F = 1$), or super-Poissonian ($F > 1$) statistics [48].

With the knowledge of the reduced density matrix of the system, we can also calculate the distribution of the photons in the resonator, which is given by the diagonal elements of ${\rm Tr}_{QD}[\hat{\rho}(t)]$ in the occupation number basis, where ${\rm Tr}_{QD}[\cdots]$ is the trace with respect to the degrees of freedom of the QD.

### C. Rotating-wave approximation

Despite its simplicity, Eq. (7) cannot be solved analytically, and it is necessary to solve it numerically. Before presenting our numerical results, it is instructive to examine the Hamiltonian of the system in a rather different representation which is more familiar in the context of the quantum optics literature [49]. By transforming to a representation in which the Hamiltonians $\hat{H}^{SC}_{dqd}$ and $\hat{H}_{\rm ph}$ are diagonal, we can find a rotating-wave approximation (RWA) description of $\hat{H}_{ph-dqd}$ from which a clear interpretation of the lasing mechanism can be obtained easily. However, the simultaneous presence of pairing ($\Gamma_S$) and tunneling ($t_d$) terms in $\hat{H}^{SC}_{dqd}$ makes its analytical diagonalization practically impossible. Nevertheless, we can use perturbation theory to obtain a unitary transformation to the lowest order in $\Gamma_S$, which can be used to obtain an approximating expression for diagonalized $\hat{H}^{SC}_{dqd}$.

We relegate the details of deriving such a unitary transformation to Appendix A, and here we solely present the results. Using a unitary transformation $\hat{U}$, whose explicit representation is given in Eq. (A6), the Hamiltonian $\hat{H}^{SC}_{dqd}$ becomes diagonalized as

$$\tilde{\hat{H}}^{SC}_{dqd} = \hat{U}^\dagger\hat{H}^{SC}_{dqd}\hat{U} = \sum_{i,\sigma} E_i\hat{\gamma}^\dagger_{i,\sigma}\hat{\gamma}_{i,\sigma} + O(\Gamma_S^2), \tag{10}$$

where $E_1(E_2) = (\varepsilon_L + \varepsilon_R)/2 \pm \{[(\varepsilon_L - \varepsilon_R)/2]^2 + t_d^2\}^{1/2}$ and the fermionic operators $\hat{\gamma}_{i,\sigma}$, with $i = 1, 2$ and $\sigma = \uparrow, \downarrow$, are related to the $\hat{d}_{i,\sigma}$ operators through Eq. (A6). By applying the same unitary transformation to the DQD-resonator coupling Hamiltonian $\hat{H}_{ph-dqd}$ and after some algebra, we reach the following expression for the transformed Hamiltonian $\tilde{\hat{H}}_{ph-dqd}$ in the rotating-wave approximation:

$$\begin{aligned}\tilde{\hat{H}}^{\rm RWA}_{ph-dqd} = uv\sum_\sigma \hat{a}\Bigg\{(g_L - g_R)\Bigg[\hat{\gamma}^\dagger_{1,\sigma}\hat{\gamma}_{2,\sigma} \\ -\Gamma_S\left(\frac{u^2}{2E_2} + \frac{v^2}{2E_1}\right)\hat{\gamma}^\dagger_{1,\sigma}\hat{\gamma}^\dagger_{2,-\sigma}\Bigg] \\ -(g_L+g_R)\Gamma_S\frac{1}{E_1+E_2}\hat{\gamma}^\dagger_{1,\sigma}\hat{\gamma}^\dagger_{2,-\sigma} + O(\Gamma_S^2)\Bigg\} + {\rm H.c.},\end{aligned} \tag{11}$$

where $u(v) = \frac{1}{\sqrt{2}}[1 \pm \frac{\varepsilon_L - \varepsilon_R}{[(\varepsilon_L-\varepsilon_R)^2+4t_d^2]^{1/2}}]^{1/2}$. Note that for $\Gamma_S = 0$, the above equation is reduced to the usual electric dipole coupling between a DQD and a resonator. We emphasis that, to the linear order of $\Gamma_S$, in addition to the term proportional to $g_L - g_R$ which is usual for the electric dipole coupling of a DQD to a resonator, there appears a new term in Eq. (11) which is proportional to $g_L + g_R$. In fact, this new, intriguing DQD-resonator coupling term is particularly due to the coupling of the superconducting lead to the DQD, and its effects were observed only very recently in Ref. [42]. Another interesting thing which we can understand from Eq. (11)

is that photon creation is accompanied by a new electronic transition in the DQD represented by the operator $\hat{\gamma}^{\dagger}_{1,\sigma}\hat{\gamma}^{\dagger}_{2,-\sigma}$, which is related to the Andreev reflections in DQD due to the coupling to the superconducting lead. It should be noted that Eq. (11) is obtained perturbatively to the first order of $\Gamma_S$, and it should not be used for a quantitative explanation of the lasing in the DQD-resonator coupled system in the general case.

### III. RESULTS AND DISCUSSION

In order to solve Eq. (7) numerically, we need to express its matrix representation in an appropriate basis. We can express the operators in Eq. (7) in the basis spanned by the states $|n_{L\uparrow}\rangle \otimes |n_{L\downarrow}\rangle \otimes |n_{R\uparrow}\rangle \otimes |n_{R\downarrow}\rangle \otimes |n_p\rangle$, where $n_{i,\sigma} = 0, 1$ is the electron occupation number and $n_p = 0, 1, 2, \ldots,$ represents the number of photons in the resonator. In practice, we need to truncate the maximum value of the photon number in the resonator to a sufficient value $n_{p,\max}$, which should be taken to be large enough to ensure the convergence of the numerical calculations. In our calculations, $n_{p,\max} = 70$ is found to be a sufficient cutoff number. It is noteworthy that to calculate the steady-state reduced density matrix, we need to solve a set of $[2^4 \times (n_{p,\max} + 1)]^2$ equations, which is a highly time and memory consuming process. The uniqueness of the calculated reduced density matrix is guaranteed by using the normalization condition $\mathrm{Tr}[\hat{\rho}(t)] = 1$. Our numerical calculations were performed by utilizing the QUTIP package [50].

Since there are no previous experiments addressing a model similar to what we consider in this work, we will take the values of our model parameters to be on the order of experimentally accessible values which are reported in some previous experimental works [42,51,52]. So we take the energy of the left dot level and the interdot tunneling energy to be $\varepsilon_L = 10\,\mu$eV and $t_d = 5\,\mu$eV. Also, we set $\Gamma_N = 0.1 \sim 1\,\mu$eV and $\Gamma_S = 1 \sim 5\,\mu$eV. The chemical potential of the superconducting electrode is taken to be the energy reference, $\mu_S = 0$, and a large positive bias voltage is applied directly to the normal electrode, $\mu_N = eV_b$. Moreover, we set the resonator damping to $\kappa = 10^{-3}\,\mu$eV and also the magnitude of the DQD-resonator coupling to $|g_L| = |g_R| = g_0 = 6.62 \times 10^{-2}\,\mu$eV. To simplify our discussion and for more clarity, we momentarily disregard the electron-electron interactions in the DQD and demonstrate the presence of the lasing state in the noninteracting case. We shall come back to the issue of the presence of nonzero electron-electron interactions in the DQD at the end of this section. In Fig. 2(a), we fix the frequency of the resonator to $\hbar\omega_0 = 13.3\,\mu$eV and plot the average photon number and the Fano factor of the photons in the resonator as a function of the energy level of the right dot $\varepsilon_R$. We see that the average photon number in the resonator shows an asymmetric peak with a maximum photon number of about $n_{\mathrm{photon}} = 20$, around $\varepsilon_R = 2.6\,\mu$eV, accompanied by a Fano factor slightly lower than $F = 1$, corresponding to a sub-Poissonian distribution of the photons in the resonator. A rigorous way to interpret why the lasing happens at this particular gate voltage and resonator frequency and also why the photon peak is asymmetric is to look at the local density of states (LDOS) of the DQD when it is in the equilibrium state and isolated from the resonator and the normal lead. The LDOS can easily

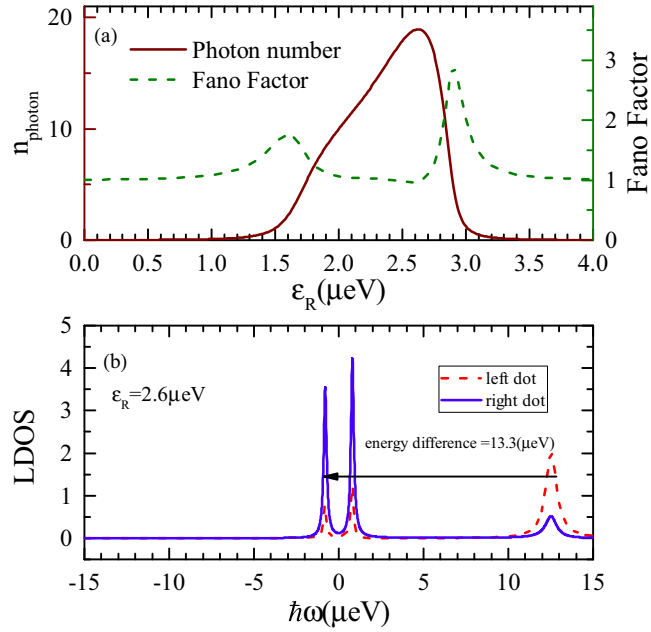


FIG. 2. (a) Average photon number (solid brown line) and Fano factor (dashed green line) as functions of the energy level of the right dot $\varepsilon_R$. (b) Local density of states of the DQD for $\varepsilon_R = 2.6\,\mu$eV. Other parameter are $\varepsilon_L = 10\,\mu$eV, $t_d = 5\,\mu$eV, $U_L = U_R = U_{LR} = 0$, $\Gamma_N = 0.1\,\mu$eV, $\Gamma_S = 1\,\mu$eV, $\mu_S = 0$, $\hbar\omega_0 = 13.3\,\mu$eV, $g_L = -g_R = g_0 = 6.62 \times 10^{-2}\,\mu$eV, and $\kappa = 10^{-3}\,\mu$eV.

be obtained from $-\mathrm{Im}[G^R_i(\omega)]$, where $G^R_i(\omega)$ is the retarded Green's function of dot $i$, which can be calculated by using the Lehmann representation (see Appendix B) [53]. In general, by coupling to a superconducting lead, the peaks in the LDOS of a QD with energies around the chemical potential of the superconducting lead will be split into two Andreev reflection subgap levels with equal but opposite sign energies [38]. On the other hand, since we have assumed a large positive bias voltage on the left lead, we can expect that the direction of electron tunnelings should be from the left to the right dot. If the energy levels of the two dots are in resonance, we will end up with an electric current originating from resonant Andreev reflections at the interface of the right dot and the superconducting lead [33,54]. However, when the energy levels of the two dots are misaligned, electron tunnelings from left to right dots are assisted by some photon excitation or absorption in the resonator, the frequency of which is equal to the energy difference between the two corresponding LDOS peaks of the left and right dots.

We plot the LDOS of the left and right dots in Fig. 2(b) for the gate voltage at which the photon number in the resonator is maximized. We see that the LDOS of the left dot has a large peak around $\hbar\omega \approx 12.3\,\mu$eV, while the LDOS of the right dot has two main peaks at energies $\hbar\omega \approx \pm 1\,\mu$eV. It can be deduced that the photon number peak in Fig. 2(a), which is for resonator frequency $\hbar\omega_0 = 13.3\,\mu$eV, is because of electron transitions between the two peaks in the LDOS of the DQD shown by an arrow in Fig. 2(b). Interestingly, we see that there is another possible electron transition with energy difference $\hbar\omega \approx 11.3\,\mu$eV, and we anticipate we can see its lasing effect by tuning the frequency of the resonator to the appropriate

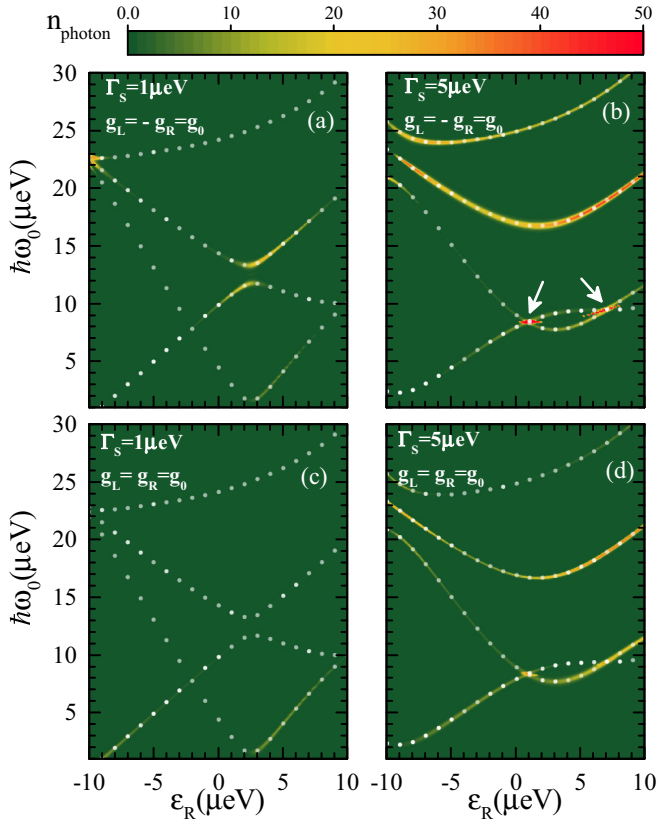


FIG. 3. (a)–(d) Average number of photons in the resonator as a function of resonator frequency $\omega_0$ and the energy level of the right dot $\varepsilon_R$ for various values of $\Gamma_S$ and $g_L$ and $g_R$. (a) $\Gamma_S = 1\,\mu$eV and $g_L = -g_R = g_0$, (b) $\Gamma_S = 5\,\mu$eV and $g_L = -g_R = g_0$, (c) $\Gamma_S = 1\,\mu$eV and $g_L = g_R = g_0$, and (d) $\Gamma_S = 5\,\mu$eV and $g_L = g_R = g_0$. White circles show the energy difference of various peaks in the LDOS at the respective $\varepsilon_R$. Other parameters are as in Fig. 2.

frequency. The origin of the asymmetry in the photon peak in Fig. 2 can also be deduced from the LDOS by noting that the weight of the Andreev subgap peaks in the LDOS is dependent on the values of the gate voltages. From the above discussion, it becomes clear that because of the presence of the superconducting lead, there is, of course, more than one possible lasing frequency in our model system corresponding to each parameter configuration of the DQD. To see this, we plot false-color plots of the average photon number in the resonator as a function of $\varepsilon_R$ and $\omega_0$ in Fig. 3. Additionally, we have also calculated energy differences between various LDOS peaks of the system at the different gate voltages, which are shown in Fig. 3 by white circles. In Fig. 3(a), we consider the same parameter configuration as in Fig. 2. We see that lasing happens at various gate voltages as well as in different resonator frequencies. Moreover, as expected, the resonator frequencies at which we can see nonzero lasing are exactly equal to the energy differences between various LDOS peaks. It is interesting to note that the regions with nonzero lasing do not follow a regular pattern, which is mainly because the positions and heights of the LDOS peaks are nonlinear functions of the values of $t_d$, $\varepsilon_R$, $\varepsilon_L$, and $\Gamma_S$. Alternatively, this nonlinearity can also be seen in the approximate expression which we obtained for the DQD-resonator coupling in Eq. (11).

Next, in Fig. 3(b), we investigate the effect of increasing the coupling energy between the right dot and the superconducting lead by setting $\Gamma_S = 5\,\mu$eV. Because of the increasing value of $\Gamma_S$, the LDOS peaks are renormalized, and therefore, their energy differences are also changed. Accordingly, the profile of the lasing which should follow these energy differences is changed as well. An important feature in Fig. 3(b) is the presence of two points, which are marked by two white arrows. We see that at these points, two branches with nonzero lasing cross, and very intriguingly, as a result of this branch crossing the photon number in the resonator is considerably increased. Actually, the crossing of two energy difference branches means that there are two distinct possible electron transitions in the LDOS with exactly the same energy difference. Hence, we can deduce that the sudden increasing of the photon number at these points is due to multiple-photon excitation due to the electron transitions from different pairs of peaks in the LDOS. Another feature in Fig. 3(b) is that, in the regions around the crossing points, some nonzero lasing occurs at frequencies which are not associated with any energy difference branches. We speculate that these nonzero lasing points originate from a two-level lasing mechanism corresponding to the electron transitions from the two nearby branches [55].

So far, in Figs. 2, 3(a), and 3(b), we have investigated the properties of the lasing state for the situation where the DQD-resonator coupling is asymmetric, where $g_L = -g_R = g_0$. However, as we have shown by using some approximative calculations in Sec. II, a spectacular character of coupling a hybrid DQD to the resonator is the presence of a new coupling mechanism which is dependent on the sum of the coupling strength of each dot to the resonator, $g_L + g_R$, and therefore, one can obtain lasing in this system even for symmetric DQD-resonator coupling as $g_L = g_R$. Thus, it is interesting to study the presence of lasing in such symmetric couplings. We have plotted in Figs. 3(c) and 3(d) the same plots as in Figs. 3(a) and 3(b), except that here, we consider the case of $g_L = g_R = g_0$. Here, because the energy configurations of the DQD are not changed, the profile of the energy differences is not altered. However, we see that there are still some nonzero lasing states available for the system in this symmetric coupling configuration. We emphasize that in the case where the DQD is coupled to two normal metals, the DQD-resonator coupling is described only by a term proportional to $g_L - g_R$, and one could expect that a symmetric DQD-resonator coupling as $g_L = g_R$ would result in a completely vanishing DQD-resonator coupling and therefore no lasing can happen in such situations.

Having realized the presence of the lasing in the coupled hybrid DQD-resonator system as well as its origins and some of its properties, we now study the effect of nonzero electron-electron interactions on the lasing state in our model system. Although it seems that the presence of finite electron-electron interactions in the hybrid-DQD could suppress the superconducting proximity correlations in the DQD and, accordingly, could reduce the lasing state, previous theoretical and experimental analysis has shown that, indeed, the electronic transport through a hybrid QD mainly depends on three

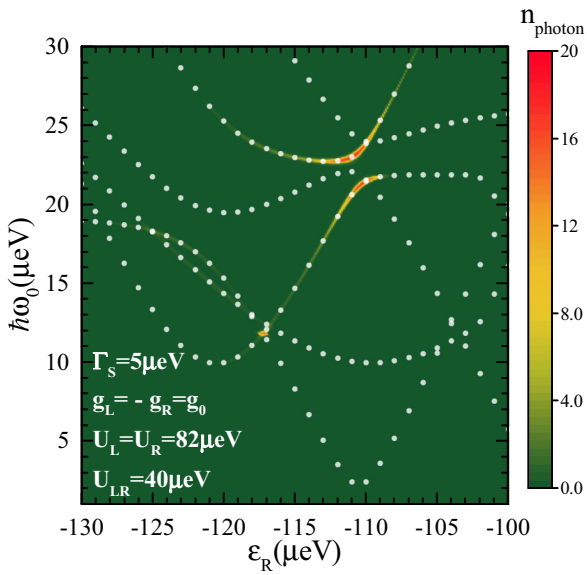


FIG. 4. Average number of photons in the resonator as a function of resonator frequency $\omega_0$ and the energy level of the right dot $\varepsilon_R$ for the presence of finite electron-electron interactions in the DQD. We set $U_L = U_R = 82\,\mu$eV and $U_{LR} = 40\,\mu$eV, and other parameters are $\varepsilon_L = -110\,\mu$eV, $t_d = 5\,\mu$eV, $\Gamma_N = 1\,\mu$eV, $\Gamma_S = 5\,\mu$eV, $\mu_S = 0$, $g_L = -g_R = g_0$, and $\kappa = 10^{-3}\,\mu$eV.

energy scales, namely, $U/\Gamma_S$, $\Gamma_N/\Gamma_S$, and $t_d/\Gamma_S$ [51,54,56]. So even for large $U$ values, we can expect nonzero conductance through the DQD, and therefore, the presence of lasing in this case is also no surprise. As a representative example, in Fig. 4, we investigate the presence of lasing for a parameter configuration like that in Fig. 3(b), except that here we consider a large electron-electron interaction in the DQD by setting $U_L = U_R = 82\,\mu$eV and $U_{LR} = 40\,\mu$eV, which are roughly similar to the values given in Ref. [42]. As a result of electron-electron interaction, the energy difference branches are split into many branches (some of them are not shown in Fig. 4), and among them, in some particular regions, we can see some nonzero lasing states in various resonator frequencies. Note the large negative gate voltages $\varepsilon_L$ and $\varepsilon_R$ applied to the DQD in Fig. 4, which are necessary to compensate the large Coulomb interactions in the DQD. Also, note that the energy difference branches are obtained from the energy differences of the roots of the retarded Green's function, which is calculated for the full interacting system by using the Lehmann representation.

## IV. CONCLUSIONS

In this paper, we studied the possibility of lasing in a single-mode electromagnetic resonator which is capacitively coupled to a hybrid DQD. We found that lasing in this system is mediated by electron tunneling between various peaks in the LDOS of the DQD which are induced by Andreev reflections at the DQD-superconducting lead's interface. Because of this particular lasing mechanism, we showed that the average photon number in the resonator in the lasing state can be further enhanced by multiple electron tunnelings between two different pairs of Andreev reflection peaks with the same energy difference in the LDOS of the DQD. Also, we showed that this system could also exhibit "two-state lasing" which is due to the electron transitions between different Andreev levels in the hybrid DQD with different energy differences.

## ACKNOWLEDGMENTS

We are grateful to F. Ebrahimi for useful discussions. Numerical calculations were performed by using high-performance computational facilities of Shahid Beheshti University (SARMAD).

## APPENDIX A: DIAGONALIZATION OF $\hat{H}^{SC}_{dqd}$

Here, we present the details of steps needed for diagonalizing the Hamiltonian $\hat{H}^{SC}_{dqd}$. In these calculations we disregard the Coulomb interaction in the DQD to simplify our presentation. We start with the matrix representation

$$\hat{H}^{SC}_{dqd} = \hat{\Psi}^\dagger (h_0 + \Gamma_S h_1)\hat{\Psi}, \tag{A1}$$

where $\hat{\Psi}^\dagger = (\hat{d}^\dagger_{1,\uparrow}, \hat{d}_{1,\downarrow}, \hat{d}^\dagger_{2,\uparrow}, \hat{d}_{2,\downarrow})$,

$$h_0 = \begin{pmatrix} \varepsilon_1 & 0 & t_d & 0 \\ 0 & -\varepsilon_1 & 0 & -t_d \\ t_d & 0 & \varepsilon_2 & 0 \\ 0 & -t_d & 0 & -\varepsilon_2 \end{pmatrix}, \tag{A2}$$

and

$$h_1 = \begin{pmatrix} 0 & 0 & 0 & 0 \\ 0 & 0 & 0 & 0 \\ 0 & 0 & 0 & 1 \\ 0 & 0 & 1 & 0 \end{pmatrix}. \tag{A3}$$

We then define four fermionic operators $\hat{\gamma}_{i,\sigma}$, with $i = 1, 2$ and $\sigma = \uparrow, \downarrow$, such that $\hat{U}^\dagger h_0 \hat{U}$ is diagonal, where $\hat{U}^\dagger = (\hat{\gamma}^\dagger_{1,\uparrow}, \hat{\gamma}_{1,\downarrow}, \hat{\gamma}^\dagger_{2,\uparrow}, \hat{\gamma}_{2,\downarrow})$. This is possible when the operators $\hat{\gamma}_{i,\sigma}$ are related to $\hat{d}_{i,\sigma}$ operators through a Bogoliubov transformation $\hat{U} = K\hat{\Psi}$, where $K$ is given by

$$K = \begin{pmatrix} u & 0 & v & 0 \\ 0 & u & 0 & v \\ -v & 0 & u & 0 \\ 0 & -v & 0 & u \end{pmatrix}, \tag{A4}$$

where

$$u(v) = \frac{1}{\sqrt{2}} \sqrt{1 \pm \frac{\varepsilon_L - \varepsilon_R}{\sqrt{(\varepsilon_L - \varepsilon_R)^2 + 4t_d^2}}}. \tag{A5}$$

Then, we find that $\hat{U}^\dagger h_0 \hat{U} = \mathrm{diag}(E_1, -E_1, E_2, -E_2)$, where $E_1(E_2) = \frac{1}{2}[\varepsilon_L + \varepsilon_R \pm \sqrt{(\varepsilon_L - \varepsilon_R)^2 + 4t_d^2}]$.

To take into account the effect of the second term in Eq. (A1), we perform a first-order perturbation on the eigenfunctions of the matrix $h_0$ with respect to the perturbation term $\Gamma_S h_1$. These perturbed eigenfunctions can be represented by

$$\hat{U} = (K + \Gamma_S K')\hat{\Psi}, \tag{A6}$$

where

$$K' = \begin{pmatrix} 0 & \frac{uv^2}{2E_1} - \frac{uv^2}{E_1+E_2} & 0 & \frac{v^3}{2E_1} + \frac{u^2v}{E_1+E_2} \\ -\frac{uv^2}{2E_1} + \frac{uv^2}{E_1+E_2} & 0 & -\frac{v^3}{2E_1} - \frac{u^2v}{E_1+E_2} & 0 \\ 0 & \frac{u^2v}{E_2+E_1} - \frac{u^2v}{2E_2} & 0 & \frac{uv^2}{E_2+E_1} + \frac{u^3}{2E_2} \\ -\frac{u^2v}{E_2+E_1} + \frac{u^2v}{2E_2} & 0 & -\frac{uv^2}{E_2+E_1} - \frac{u^3}{2E_2} & 0 \end{pmatrix}. \tag{A7}$$

Now, it is straightforward to show by matrix multiplication that the first-order correction to the eigenenergies of $\hat{H}^{SC}_{dqd}$ is zero, and its diagonalized form in terms of $\hat{\gamma}_{i,\sigma}$ operators can be given by

$$\tilde{\hat{H}}^{SC}_{dqd} = U^\dagger \hat{H}^{SC}_{dqd} U = \sum_{i,\sigma} E_i \hat{\gamma}^\dagger_{i,\sigma} \hat{\gamma}_{i,\sigma} + O(\Gamma_S^2). \tag{A8}$$

The main benefit which we can obtain from the above calculations is that we can apply the same unitary transformation $U$ on the DQD-resonator coupling Hamiltonian $\hat{H}_{ph-dqd}$ to obtain its representation in terms of $\hat{\gamma}_{i,\sigma}$ operators as

$$\begin{aligned} &\tilde{\hat{H}}_{ph-dqd} \\ &= -\sum_\sigma (\hat{a} + \hat{a}^\dagger) \Bigg\{ (g_L - g_R) \\ &\quad \times \left[ -uv \hat{\gamma}^\dagger_{1,\sigma} \hat{\gamma}_{2,\sigma} + \Gamma_S uv \left( \frac{u^2}{2E_2} + \frac{v^2}{2E_1} \right) \hat{\gamma}^\dagger_{1,\sigma} \hat{\gamma}^\dagger_{2,-\sigma} \right] \\ &\quad - (g_L + g_R) \left[ \Gamma_S \frac{uv}{E_1 + E_2} \hat{\gamma}^\dagger_{1,\sigma} \hat{\gamma}^\dagger_{2,-\sigma} \right] \Bigg\} + \text{H.c.} \end{aligned} \tag{A9}$$

## APPENDIX B: LEHMANN REPRESENTATION OF $G^R_i(\omega)$

As we discussed in Sec. III, to the linear order of interaction between the DQD and the resonator and in the weak-coupling regime, it is reasonable to expect that the possible lasing frequencies in the resonator can be explained by electron transitions between various peaks in the LDOS of the DQD when it is isolated from the resonator and also from the normal lead. It is convenient to calculate the LDOS of the DQD from $-\text{Im}[G^R_i(\omega)]$, where $G^R_i(\omega)$ is the retarded Green's function of dot $i$ and can be calculated from the Lehmann representation [53]. In the following we briefly summarize the main steps needed to calculate the retarded Green's function of the DQD.

Our starting point is the Hamiltonian of the DQD,

$$\begin{aligned} \hat{H}^{SC}_{dqd} = &\sum_{\alpha\sigma} \varepsilon_\alpha \hat{n}_{\alpha,\sigma} + U_\alpha \hat{n}_{\alpha,\uparrow} \hat{n}_{\alpha,\downarrow} + U_{LR} \hat{n}_L \hat{n}_R \\ &+ t_d \sum_\sigma (d^\dagger_{R,\sigma} d_{L,\sigma} + \text{H.c.}) + \Gamma_S (\hat{d}^\dagger_{R,\uparrow} \hat{d}^\dagger_{R,\downarrow} + \text{H.c.}). \end{aligned} \tag{B1}$$

To proceed, we need the eigenstates and the eigenenergies of Eq. (B1), for which, as we discussed in Sec. II, obtaining an analytical expression for its eigenstates is practically impossible. Nevertheless, we can rely on numerical methods and express the numerically calculated eigenstates of Eq. (B1) and their corresponding eigenenergies by $|n\rangle$ and $\mathcal{E}_n$, where $n = 1, 2, \ldots, 16$. Having the eigenspectrum of the Hamiltonian of the DQD, we can then calculate the retarded Green's function of the DQD from

$$G^R_{i,\sigma}(\omega) = \frac{1}{Z} \sum_{m,m'} \frac{\langle m | d_{i,\sigma} | m' \rangle \langle m' | d^\dagger_{i,\sigma} | m \rangle}{\omega + \mathcal{E}_m - \mathcal{E}_{m'} + i\eta} \left( e^{-\beta \mathcal{E}_m} + e^{-\beta \mathcal{E}_{m'}} \right), \tag{B2}$$

where $Z = \sum_m e^{-\beta \mathcal{E}_m}$, $\eta$ is an infinitesimal positive constant, and $\beta$ is the inverse temperature.


[1] Y. Mu and C. M. Savage, Phys. Rev. A **46**, 5944 (1992).
[2] C. Ginzel, H.-J. Briegel, U. Martini, B.-G. Englert, and A. Schenzle, Phys. Rev. A **48**, 732 (1993).
[3] T. Pellizzari and H. Ritsch, Phys. Rev. Lett. **72**, 3973 (1994).
[4] T. Pellizzari and H. Ritsch, J. Mod. Opt. **41**, 609 (1994).
[5] K. An, J. J. Childs, R. R. Dasari, and M. S. Feld, Phys. Rev. Lett. **73**, 3375 (1994).
[6] B. Jones, S. Ghose, J. P. Clemens, P. R. Rice, and L. M. Pedrotti, Phys. Rev. A **60**, 3267 (1999).
[7] M. Löffler, G. M. Meyer, and H. Walther, Phys. Rev. A **55**, 3923 (1997).
[8] T. Karlovich and S. Y. Kilin, Opt. Spectrosc. **91**, 343 (2001).
[9] J. McKeever, A. Boca, A. D. Boozer, J. R. Buck, and H. J. Kimble, Nature (London) **425**, 268 (2003).
[10] T. Yoshie, A. Scherer, J. Hendrickson, G. Khitrova, H. Gibbs, G. Rupper, C. Ell, O. Shchekin, and D. Deppe, Nature (London) **432**, 200 (2004).
[11] L. Florescu, S. John, T. Quang, and R. Wang, Phys. Rev. A **69**, 013816 (2004).
[12] T. Aoki, B. Dayan, E. Wilcut, W. P. Bowen, A. S. Parkins, T. Kippenberg, K. Vahala, and H. Kimble, Nature (London) **443**, 671 (2006).
[13] P. Lougovski, F. Casagrande, A. Lulli, and E. Solano, Phys. Rev. A **76**, 033802 (2007).
[14] L. Florescu, Phys. Rev. A **78**, 023827 (2008).
[15] H.-J. Kim, A. H. Khosa, H.-W. Lee, and M. S. Zubairy, Phys. Rev. A **77**, 023817 (2008).
[16] S. Ritter, P. Gartner, C. Gies, and F. Jahnke, Opt. Express **18**, 9909 (2010).
[17] J. P. Reithmaier, G. Sek, A. Löffler, C. Hofmann, S. Kuhn, S. Reitzenstein, L. Keldysh, V. Kulakovskii, T. Reinecke, and A. Forchel, Nature (London) **432**, 197 (2004).
[18] S. Reitzenstein, C. Böckler, A. Bazhenov, A. Gorbunov, A. Löffler, M. Kamp, V. Kulakovskii, and A. Forchel, Opt. Express **16**, 4848 (2008).
[19] M. Nomura, N. Kumagai, S. Iwamoto, Y. Ota, and Y. Arakawa, Opt. Express **17**, 15975 (2009).
[20] M. Nomura, N. Kumagai, S. Iwamoto, Y. Ota, and Y. Arakawa, Nat. Phys. **6**, 279 (2010).
[21] N. Ledentsov, Semicond. Sci. Technol. **26**, 014001 (2010).
[22] H. Liu, T. Wang, Q. Jiang, R. Hogg, F. Tutu, F. Pozzi, and A. Seeds, Nat. Photonics **5**, 416 (2011).
[23] M. Marthaler, Y. Utsumi, D. S. Golubev, A. Shnirman, and G. Schön, Phys. Rev. Lett. **107**, 093901 (2011).

[24] P.-Q. Jin, M. Marthaler, J. H. Cole, A. Shnirman, and G. Schön, Phys. Rev. B **84**, 035322 (2011).
[25] H. Toida, T. Nakajima, and S. Komiyama, Phys. Rev. Lett. **110**, 066802 (2013).
[26] Y.-Y. Liu, J. Stehlik, C. Eichler, M. Gullans, J. M. Taylor, and J. Petta, Science **347**, 285 (2015).
[27] C. Karlewski, A. Heimes, and G. Schön, Phys. Rev. B **93**, 045314 (2016).
[28] J. Stehlik, Y.-Y. Liu, C. Eichler, T. R. Hartke, X. Mi, M. J. Gullans, J. M. Taylor, and J. R. Petta, Phys. Rev. X **6**, 041027 (2016).
[29] O. Astafiev, K. Inomata, A. Niskanen, T. Yamamoto, Y. A. Pashkin, Y. Nakamura, and J. Tsai, Nature (London) **449**, 588 (2007).
[30] J. Hauss, A. Fedorov, C. Hutter, A. Shnirman, and G. Schön, Phys. Rev. Lett. **100**, 037003 (2008).
[31] M. Grajcar, S. Van der Ploeg, A. Izmalkov, E. Ilichev, H.-G. Meyer, A. Fedorov, A. Shnirman, and G. Schön, Nat. Phys. **4**, 612 (2008).
[32] S. André, V. Brosco, M. Marthaler, A. Shnirman, and G. Schön, Phys. Scr. **T137**, 014016 (2009).
[33] Q.-F. Sun, J. Wang, and T.-H. Lin, Phys. Rev. B **59**, 3831 (1999).
[34] Q.-F. Sun, J. Wang, and T.-H. Lin, Phys. Rev. B **59**, 13126 (1999).
[35] Q.-F. Sun, H. Guo, and T.-H. Lin, Phys. Rev. Lett. **87**, 176601 (2001).
[36] J. C. Cuevas, A. Levy Yeyati, and A. Martín-Rodero, Phys. Rev. B **63**, 094515 (2001).
[37] A. Nurbawono, Y. P. Feng, and C. Zhang, Phys. Rev. B **82**, 014535 (2010).
[38] J. Barański and T. Domański, J. Phys.: Condens. Matter **25**, 435305 (2013).
[39] I. Weymann and K. P. Wójcik, Phys. Rev. B **92**, 245307 (2015).
[40] L. E. Bruhat, J. J. Viennot, M. C. Dartiailh, M. M. Desjardins, T. Kontos, and A. Cottet, Phys. Rev. X **6**, 021014 (2016).
[41] G. Rastelli and M. Governale, Phys. Rev. B **100**, 085435 (2019).
[42] L. E. Bruhat, T. Cubaynes, J. J. Viennot, M. C. Dartiailh, M. M. Desjardins, A. Cottet, and T. Kontos, Phys. Rev. B **98**, 155313 (2018).
[43] P. Trocha and J. Barnaś, Phys. Rev. B **89**, 245418 (2014).
[44] S. E. Nigg, R. P. Tiwari, S. Walter, and T. L. Schmidt, Phys. Rev. B **91**, 094516 (2015).
[45] M. J. Gullans, J. M. Taylor, and J. R. Petta, Phys. Rev. B **97**, 035305 (2018).
[46] B. K. Agarwalla, M. Kulkarni, and D. Segal, Phys. Rev. B **100**, 035412 (2019).
[47] S. Pfaller, A. Donarini, and M. Grifoni, Phys. Rev. B **87**, 155439 (2013).
[48] U. C. Mendes and C. Mora, Phys. Rev. B **93**, 235450 (2016).
[49] H.-P. Breuer and F. Petruccione, *The Theory of Open Quantum Systems* (Oxford University Press, Oxford, 2002).
[50] J. R. Johansson, P. D. Nation, and F. Nori, Comput. Phys. Commun. **184**, 1234 (2013).
[51] Y.-J. Doh, S. D. Franceschi, E. P. Bakkers, and L. P. Kouwenhoven, Nano Lett. **8**, 4098 (2008).
[52] Y.-Y. Liu, K. D. Petersson, J. Stehlik, J. M. Taylor, and J. R. Petta, Phys. Rev. Lett. **113**, 036801 (2014).
[53] H. Bruus and K. Flensberg, *Many-Body Quantum Theory in Condensed Matter Physics: An Introduction* (Oxford University Press, Oxford, 2004).
[54] Y. Tanaka, N. Kawakami, and A. Oguri, Phys. Rev. B **81**, 075404 (2010).
[55] A. Markus, J. Chen, C. Paranthoen, A. Fiore, C. Platz, and O. Gauthier-Lafaye, Appl. Phys. Lett. **82**, 1818 (2003).
[56] R. S. Deacon, Y. Tanaka, A. Oiwa, R. Sakano, K. Yoshida, K. Shibata, K. Hirakawa, and S. Tarucha, Phys. Rev. Lett. **104**, 076805 (2010).